International Journal of Thermophysics, Vol. 16, No. 2, 1995

Simulation and SANS Studies of Gelation Under Shear[1]

C. D. Muzny,[2] D. Hansen,[3] G. C. Straty,[4] D. J. Evans,[3] and H. J. M. Hanley[3,4,5]

Computer simulations of a two-dimensional Lennard-Jones fluid undergoing spinodal decomposition are reported for the system subjected to planar Couette flow. Key results are the images of the atomic structure and plots of the corresponding pair correlation functions. A companion small-angle neutron scattering (SANS) study of shear-influenced gelation in colloidal silica suspensions at volume fractions $\phi = 0.1$, 0.12, 0.18, and 0.24 is discussed. It is found that the scattered intensity–wave vector curves from the unsheared gels obey a power law for $\phi < 0.24$. At higher volume fractions, the power law does not seem to be followed. Shear, however, induces an apparent fractal structure in the gel at $\phi = 0.24$. Results from the computer and the SANS experiments indicate that the spinodal decomposition process and the gelation mechanism have features in common.

KEY WORDS: colloidal silica; gelation; Lennard-Jones fluid; nonequilibrium molecular dynamics; shear; small-angle neutron scattering; spinodal decomposition; structure factor; two-dimensional fluid.

1. INTRODUCTION

Brinker and Scherer [1] define a gel as a continuous solid skeleton enclosing a continuous liquid phase. One can also consider a gel as a mechanically

[1] Paper presented at the Twelfth Symposium on Thermophysical Properties, June 19–24, 1994, Boulder, Colorado, U.S.A.

[2] Condensed Matter Laboratory, Department of Physics, University of Colorado, Boulder, Colorado 80303, U.S.A.

[3] Research School of Chemistry, Australian National University, Canberra, Australia.

[4] Thermophysics Division, National Institute of Standards and Technology, Boulder, Colorado 80303, U.S.A.

[5] Author to whom correspondence should be addressed.

0195-928X/95/0300-0337$07.50/0

and thermodynamically unstable microscopic network made up of some defined unit, e.g., a particle or segment of a polymer chain. Instability is frozen when the network growth and/or rearrangement is restricted by the finite size of the gel's container and the experimental conditions. Experiment supports this view; for example, (a) a suspension can be gelled very slowly, giving either an amorphous liquid-like solid phase (as for a slowly dried silica gel [2]), or a crystal (as in opal formation [3]), and (b) on aging, a gel can rearrange to a metastable amorphous solid, or to a stable crystal [1]. In a later paper [4] we will argue that the growth of a gel must have features in common with spinodal decomposition. Here, as a preliminary, the spinodal behavior [5, 6][6] of a two-dimensional Lennard-Jones fluid is explored. To see how this phenomenon might parallel reaction-limited gelation, the results are compared and contrasted with recently reported small-angle neutron scattering (SANS) data on the gelation of an aqueous silica suspension [7].

Both the simulation and the SANS experiments were carried out with a system subjected to an applied shear. We know that shear must influence thermodynamic stability [4]; shear must, therefore, influence the gelation process. An objective of this paper is to investigate this.

2. COMPUTER SIMULATION

The computer simulation was based on the nonequilibrium molecular dynamic (NEMD) procedure discussed extensively by Evans and co-workers [8, 9]. Details of the algorithms will not be given, but in essence, a model system is studied under an applied shear rate, γ, while thermostatted to a constant temperature, T. Here, a Lennard-Jones two-dimensional fluid of N particles of mass m was set up by assigning initial values of the positions and peculiar momenta, $\mathbf{r}_i$ and $\mathbf{p}_i$ ($i = 1, N$), in area A bounded by periodic boundaries. The density, $\rho = N/A$, was given as an input variable, and a value designated for the kinetic temperature. (As usual in a simulation, all variables are reduced by the mass and the potential parameters, σ_{LJ} and ε_{LJ}, which are, in turn, set equal to one.) The behavior of the fluid was investigated when isolated and when subjected to planar Couette flow, at a shear rate defined by $\gamma = \partial u_x/\partial y$, with u_x the x component of the peculiar velocity. The algorithm solves the thermostatted SLLOD equations of motion [9]:

[6] Ref. 5 points out that a fluid quenched into the unstable part of the gas–liquid phase diagram will decay to the coexisting equilibrium gas and liquid phases and form highly interconnected regions, with densities slightly above and slightly below the assigned density, during the decomposition.

$$\frac{d\mathbf{r}_i}{dt} = \frac{\mathbf{p}_i}{m} + \mathbf{n}_x \dot{\gamma} y_i \tag{1}$$

$$\frac{d\mathbf{p}_i}{dt} = \mathbf{F}_i - \mathbf{n}_x \dot{\gamma} p_{iy} - \alpha \mathbf{p}_i \tag{2}$$

where $\mathbf{n}_x$ is the unit vector in the flow direction. In Eq. (2), the force, $\mathbf{F}_i = -\sum_j \partial\phi_{LJ}(r)/\partial\mathbf{r}_i$, where ϕ_{LJ} is the potential between particles i and j, with $r = |\mathbf{r}_i - \mathbf{r}_j|$. The simulations were always run at low Reynolds numbers, hence the peculiar velocity of any particle i is given unambiguously by Eq. (1) and the kinetic temperature is defined in the usual way; namely, by $T = \sum_i (\mathbf{p}_i^2)/2mNk_B$, where k_B is Boltzmann's constant. The equations include the thermostatting multiplier, α, given by

$$\alpha = \sum_{i=1}^{N} \mathbf{p}_i \cdot \mathbf{F}_i \Big/ \sum_{i=1}^{N} \mathbf{p}_i \cdot \mathbf{p}_i \tag{3}$$

to ensure that T is constant. Note that for shear, the boundaries are modified to satisfy the Lees–Edwards "sliding brick" conditions [8–10] in which periodic images of the simulation cell above and below the unit cell are moved in opposite directions at a velocity determined by the imposed shear rate.

Simulations were carried out with $N = 3584$, with the ϕ_{LJ} truncated at $2.5\sigma_{LJ}$. The time step was set at $\Delta t = 0.004$ and the simulation monitored over at least 250,000 time steps. The system was equilibrated in the liquid at $\rho = 0.325$ and $T = 1.0$ [5, 11] and then quenched into the unstable region to a state point of $\rho = 0.325$ and $T = 0.45$. Given the record of particle positions as a function of time, the properties of the two-dimensional fluid were evaluated in the usual way [9]. However, the feature of interest for this study was the atomic morphology—or microstructure—represented by two-dimensional images of the atomic positions at various times during a simulation run and by the variation of the pair correlation function $g(r)$. Data were extracted for the unsheared system, and for the system when subjected to a shear rate of $\dot{\gamma} = 0.1$.

2.1. Results

2.1.1. Unsheared System

The two-dimensional image in Fig. 1a depicts the atomic configuration for $t = 1000$ after the quench. Figure 2 shows the corresponding pair correlation function plotted logarithmically as a function of the distance r/σ. That the decomposition, even the gas/liquid decomposition, has

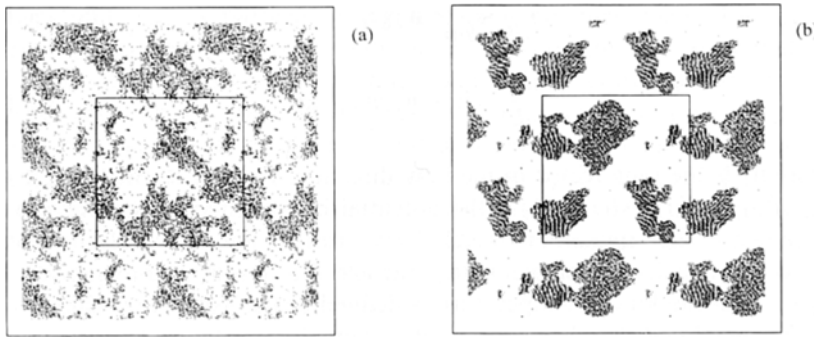

Fig. 1. (a) Atomic configurations from a spinodally decomposing two-dimensional Lennard-Jones fluid at $t = 1000$ after quenching. See text. The central square outlines the unit simulation cell about which the structure is repeated periodically. (b) The configurations at $t = 1000$ after the quench with the system subjected to a shear of 0.1.

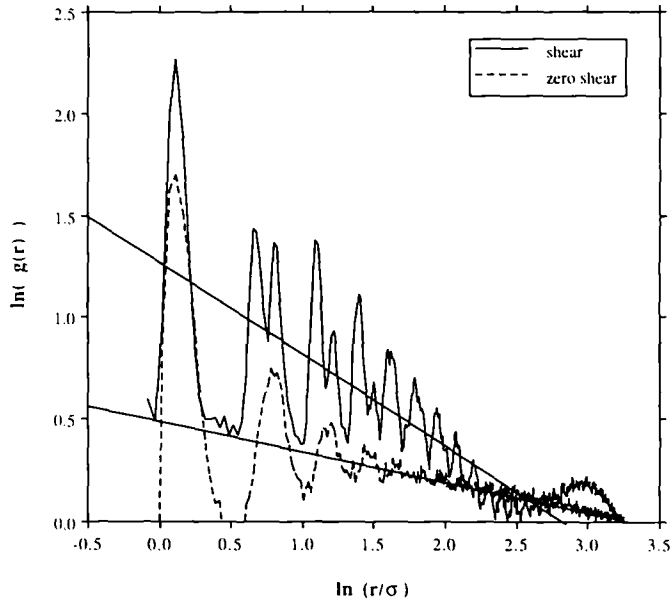

Fig. 2. Pair correlation functions for the unsheared and sheared system corresponding to Figs. 1a and 1b. Note the decays (indicated by the straight lines) with $\ln(r\,\sigma)$ and the enhanced structure evident in the sheared system.

features of gel formation is very clear. Figure 1a has at least the superficial features of gel structure [1] and resembles the two-dimensional gelation images of Armstrong et al. [12] and of Hurd and Schaefer [13]. Figure 2 indicates long-range order consistent with the known tendency of gels to form a fractal [14]; $g(r)$ oscillates above one and $g(r) = 1$ only at long r. The decay has an approximate linear region and is not inconsistent with the properties of a fractal for which $g(r) \sim r^{d-3}$, where d is the fractal dimension. [The relation between the possible fractal nature of the particle morphology and the exponent is discussed in Ref. 4.]

The radial distribution function was Fourier-transformed to give an estimate of the structure factor $S(Q\sigma)$. We confirmed that the plots of $S(Q\sigma)$ were close to those reported by Koch et al. [5]; they are not shown here. The plots indicate that the structure of the prequenched liquid is absent. However, there is a weak peak at $Q\sigma \approx 2\pi$, indicating the particles are in contact.

2.1.2. Sheared System

Figure 1b displays the atomic morphology for the system subjected to the shear of 0.1 at $t = 1000$ postquench; Fig. 2 shows the corresponding plots for $g(r)$. Significant differences between the data sets are seen. Shear has caused large, elongated clumps to form and has increased the slope of the linear decay seen in Fig. 2 (and enhanced the particle contact peak at $Q \approx 2\pi$). Figure 2 shows that short-range order in the sheared system is more evident than in the unsheared equivalent; in fact, the pair correlation function indicates features of the solid.

3. SMALL-ANGLE NEUTRON SCATTERING

The SANS study [7] was carried out on the 30-m instruments at the NIST Cold Neutron Research Facility. The first series of experiments measured the scattering intensity from ungelled colloidal silica suspensions of volume fractions $\phi = 0.1$, 0.12, 0.18, and 0.24 prepared in a H_2O/D_2O (30%) medium from a stock solution of Ludox TM-50, silica particles[7] of nominal diameter $\sigma = 22$ nm. A suspension was placed in a quartz cell of path length 1 mm and the spectrometer configured to a wavelength $\lambda = 0.6$ nm and sample-to-detector distances of 15, 13, 8, 5, and 2 m. We measured the scattered intensities, $I(Q)$, as a function of the scattered wave vector $Q = (4\pi/\lambda) \sin \theta/2$, where λ is the incident neutron wavelength and θ the scattering angle. The data were corrected for the cell background and detector variation and put on an absolute scale. Single-particle form-factor

[7] The trade name is used to identify the product, and implies no NIST endorsement.

data were measured from a suspension at $\phi = 0.0025$ and the result checked against a theoretical polydisperse form factor modified to allow for instrument smearing [15]. The diameter was estimated to be $\sigma = 24$ nm, with a polydispersity of 15%.

Gelation was induced by adjusting the pH of the suspensions to 5.8 ± 0.1 with 0.1 M HCl, with NaCl added to give a solution of 0.4 M NaCl. An alternate gel at $\phi = 0.24$ was made without salt to explore the effect of a different gelation mechanism on the final gel structure. Scattered intensity data were obtained from the gelled samples in the quartz cells, and the data analyzed as before. The gelation process was assumed complete when the measured intensity was time independent and we found this took from 6 h for the dense suspension to 12 h for the dilute. Gelation at $\phi = 0.1$ was monitored by measuring the intensities at 10-min intervals for 3 h, then hourly for a further 9 h after gelation initiation.

For the shear studies, the SANS instrument was configured at 13 m at a wavelength of 0.6 nm with the NIST 1-mm-gap-width Couette shearing cell [16] in the sample position. (In our coordinate system with the incident beam along the y direction, the flow velocity $\mathbf{u}$ is along the x direction, and the shear rate is defined as $\dot{\gamma} = \partial u_x / \partial y$.) A gelation-initiated sample was loaded into the Couette cell, subjected to a shear rate of $\dot{\gamma} = 4500\ \mathrm{s}^{-1}$, and the scattered intensity was then monitored. A sector average of the sheared intensities in the x–z plane of the detector showed some anisotropy at the higher volume fractions. This, however, was very weak and the data were circularly averaged and reduced following the procedure for the unsheared suspensions and gels. Intensities were measured at regular intervals until the scattering pattern from the shearing system was time independent. At this point the shear was removed and the intensity remeasured. Only very small relaxation was noted; in effect, the intensity did not change significantly.

3.1. Results

3.1.1. Unsheared Gels

The main features of the final gelation data for the isolated systems are displayed in Figs. 3 and 4. Figure 3 shows sample scattered intensities for volume fractions 0.12 and 0.24 (gelled with NaCl), together with the intensity from the ungelled sol at $\phi = 0.12$. Figure 4 is a plot of the structure factors for these systems. One sees:

1. The scattered intensities in Fig. 3 must reflect form-factor scattering at high $Q\sigma$, since $S(Q\sigma)$ tends to 1, and we see that the curves essentially superimpose if $\ln(Q\sigma) > 1.75$. We thus conclude that the basic unit of

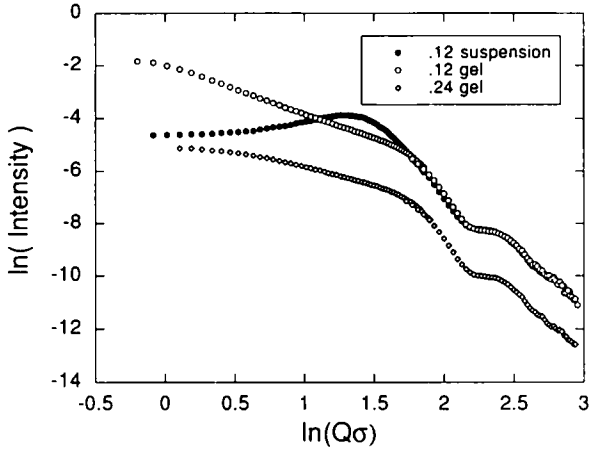

Fig. 3. SANS intensities, in arbitrary units, from colloidal silica gels compared with the intensity of the suspension at $\phi = 0.12$.

the gelling system (here the Ludox particle of diameter 24 nm) remains unchanged during gelation, hence validating our procedure to extract a structure factor from the geled system by dividing out the form factor.

2. The peak associated with the suspension is suppressed on gelation, but there is evidence of a weak peak at $Q\sigma \approx 2\pi$.

3. Figure 4 shows that the gel at $\phi = 0.24$ has no distinctive features at low Q. Contrast the curve for this volume fraction with that for $\phi = 0.12$,

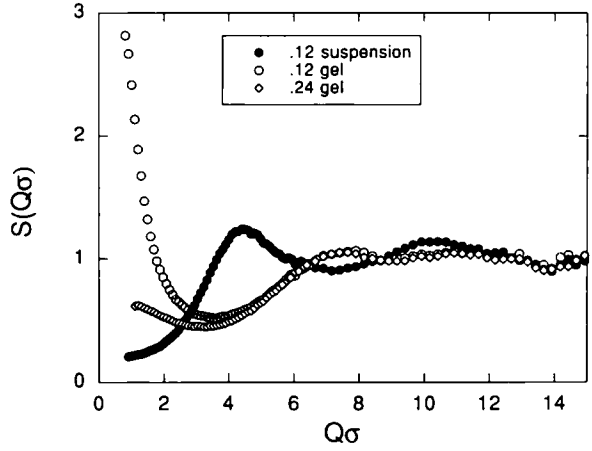

Fig. 4. The structure factors for the gels and suspension of Fig. 3.

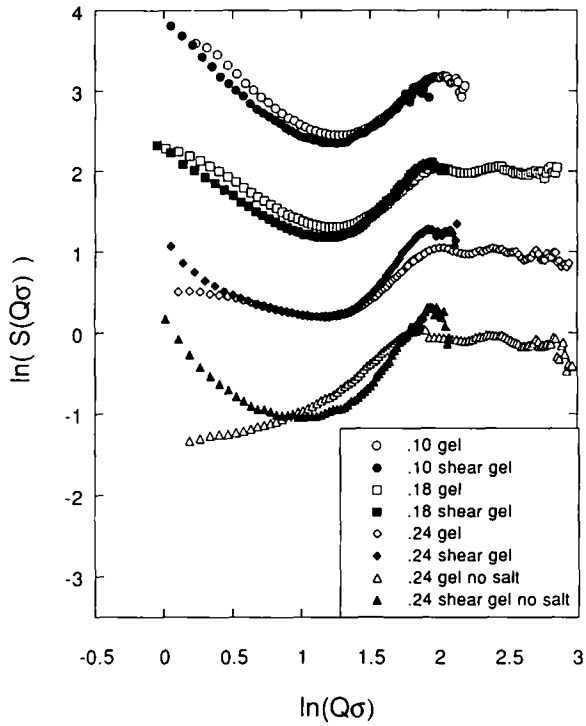

Fig. 5. Structure factors of sheared gels compared with their unsheared equivalents. Note that shear has extended the linear region at low Q for $\phi = 0.10$ and 0.18 and induced long-range order in the $\phi = 0.24$ systems. The effect of shear on the 0.24 (no salt) sample is particularly noticeable.

where, in fact, the linear portion of the intensity curve at $\phi = 0.12$ obeys a power law. That silica gels can be fractal is well known [14, 17], but our systems are at higher volume fractions than those investigated in the past [17, 18]. A log-log plot at $\phi = 0.10$ (Fig. 5) gives a power law slope $d = 1.94 \pm 0.03$. This apparent dimension is slightly lower than the expected value of 2.1 estimated from the reaction-limited cluster–cluster model [14], and substantially lower than the value of 2.4 found from previous studies of silica gels at moderate volume fractions [18]. Reasons for the possible discrepancies will be explored in further work [4]. Note that we have not attempted a proper fit of the possible fractal regions, since the SANS data do not extend to a sufficiently low Q to estimate reliably the fractal correlation length, ζ. See Ref. 7.

3.1.2. Shear Gels

Shear impacts strongly on gel structure at the volume fractions of interest here. Figure 5 displays the structure factors for $\phi = 0.10$, 0.18, and 0.24 (gelled with and without NaCl). Shear has extended the linear domain in the structure factor at lower Q for $\phi = 0.10$ and 0.18. Shear has induced a long-range correlation into the gel structures at $\phi = 0.24$. Shear has also enhanced the peak at $Q \approx 2\pi$, even at the lower fraction.

In summary, the SANS results are consistent with the picture of the unsheared silica particulate gel as a filamentary structure in which the particles are essentially in contact for $\phi = 0.10$ and 0.18. Under shear, however, the filamentary nature of the gel is enhanced, in fact induced, at $\phi = 0.24$, especially in the sample gelled without NaCl.

4. COMPARISONS AND CONCLUSIONS

A simulation of a two-dimensional fluid undergoing spinodal decomposition has been discussed. Atomic configurations and the corresponding pair correlation functions are presented for a system when isolated and when subjected to a shear. Data from a SANS study of gelling silica suspensions are also reported. Conclusions are: First, that the computer simulation and the experiments give results that have very much in common. The exact connection between spinodal decomposition and gelation will be deferred, however, until further simulations on the solid/gas decomposition have been completed. Second, both the simulation and the SANS experiments indicate that the action of the shear can have a profound effect on the long-range structure, and can enhance the short-range packing.

ACKNOWLEDGMENTS

The work was supported in part by a grant from the Office of Basic Energy Sciences, Division of Engineering and Geosciences, U.S. Department of Energy. We are grateful to Aneta Lewandowski for help with the sample preparations, and grateful to the staff of the NIST Cold Neutron Research Facility for their advice and encouragement. D.H. and D.J.E. would like to thank Fujitsu, the ANU Computer Science Department, and the ANU Supercomputer Facility for generous grants of computing time. We are also grateful to William O. Roberts, Du Pont, for supplying the silica samples and for valuable discussions.

REFERENCES

1. C. J. Brinker and G. W. Scherer, *Sol-Gel Science* (Academic Press, Boston, 1990).
2. J. D. F. Ramsay and B. O. Booth, *J. Chem. Soc. Faraday Trans. 1* **79**:173 (1983).
3. J. V. Sanders and M. J. Murray, *Philos. Mag.* **42**:721 (1980).
4. B. D. Butler, H. J. M. Hanley, D. Hansen, and D. J. Evans, in press (1995).
5. S. W. Koch, R. C. Desai, and F. F. Abraham, *Phys. Rev. A* **27**:2152 (1983).
6. M. Carpinetti and M. Giglio, *Phys. Rev. Lett.* **68**:3327 (1992); P. W. Rouw, A. T. J. M. Woutersen, B. J. Ackerson, and C. G. De Kruif, *Physica A* **156**:876 (1989); R. W. Pekala and D. W. Schaefer, *Macromolecules* **26**:5487 (1993).
7. C. D. Muzny, G. C. Straty, and H. J. M. Hanley, *Phys. Rev. E* **50**:R675 (1994).
8. D. J. Evans and G. P. Morriss, *Computer Phys. Rep.* **1**:297 (1984).
9. D. J. Evans and G. P. Morriss, *Statistical Mechanics of Nonequilibrium Fluids* (Academic Press, London, 1990).
10. A. W. Lees and S. F. Edwards, *J. Phys. C* **5**:1921 (1972).
11. J. A. Barker, D. Henderson, and F. F. Abraham, *Physica* **106**:226 (1981).
12. A. J. Armstrong, R. C. Mockler, and W. J. O'Sullivan, *J. Phys. A: Math. Gen.* **19**:1123 (1986).
13. A. J. Hurd and D. W. Schaefer, *Phys. Rev. Lett.* **54**:1043 (1985).
14. J. E. Martin and A. J. Hurd, *J. Appl. Cryst.* **20**:61 (1987).
15. P. van Beurten and A. Vrij, *J. Chem. Phys.* **74**:2744 (1981).
16. G. C. Straty, *NIST J. Res.* **94**:259 (1989); G. C. Straty, H. J. M. Hanley, and C. J. Glinka, *J. Stat. Phys.* **62**:1015 (1991).
17. G. Dietler, C. Aubert, D. S. Cannell, and P. Wiltzius, *Phys. Rev. Lett.* **57**:3117 (1986); F. Ferri, B. J. Frisken, and D. S. Cannell, *Phys. Rev. Lett.* **67**:3626 (1991), and references therein.
18. M. Foret, J. Pelous, R. Vacher, and J. Marignam, *J. Non-Cryst. Solids* **145**:133 (1992).